Mineralogical Magazine, August 2006, Vol. 70(4), pp. 445–457

An investigation of extreme silver enrichment at tennantite surfaces exposed to alkaline solutions: an XPS-based study

E. L. HOBSON*, P. WINCOTT, D. J. VAUGHAN AND R. A. D. PATTRICK

School of Earth, Atmospheric and Environmental Sciences, and Williamson Research Centre for Molecular Environmental Science, University of Manchester, Oxford Road, Manchester M13 9PL, UK

ABSTRACT

Extreme silver enrichment at the surface of the complex sulphide, tennantite (ideal formula: $Cu_{12}As_4S_{13}$), occurs following exposure to alkaline solutions, and involves the development of an Ag-rich sulphide surface species. The tennantite has a low bulk Ag content of 0.3 at.%, and a percentage surface enrichment of Ag is thirty-six times that of the bulk. The techniques of X-ray photoelectron spectroscopy (XPS) and reflection extended X-ray absorption fine structure spectroscopy show the new phase to be a Ag sulphide species compositionally similar to cupriferous proustite ($(Cu,Ag)_3AsS_3$). Solution experiments and XPS depth profiling show that the surface is most depleted in Cu and Zn, and enriched in Ag compared to the bulk tennantite. Selective dissolution and reprecipitation at the tennantite surface cannot explain the enrichment of Ag relative to the bulk. Migration must have occurred and could have been driven by the leaching out of Cu which produces a metal-depleted surface, coupled to the relative incompatibility of Ag in the tennantite lattice. To account for the extreme enrichment at the surface, Ag must have diffused from depths of up to 9 nm, probably via structural weaknesses and vacancies in the tennantite lattice.

KEYWORDS: tennantite, tetrahedrite, Ag, diffusion, migration, enrichment, XPS, leaching, alkaline solutions, surface, REFLEXAFS.

Introduction

THE study of mineral surfaces is critical to understanding the behaviour of minerals during the processes used in mineral separation and concentration, especially froth flotation and leaching. The flotation characteristics of sulphides are strongly dependent on the surface species present and a particular problem with sulphides during flotation is the unwanted adsorption of species present in solution onto the surfaces of the minerals, resulting in a change in their flotation responses. An additional difficulty is predicting the flotation responses for chemically complex sulphides, such as the tetrahedrite–tennantite group, where the active surface species are poorly defined. The degree of surface oxidation can also radically change the species and chemistry at the mineral surface. Of particular interest to sulphide mineral flotation is the behaviour in alkaline solutions, especially high pH (>10) hydroxide-bearing solutions as these are the most widely used moderators of flotation cell conditions (Wills, 1997).

In this paper, a significant modification to the surface of the complex sulphide mineral tennantite (ideal formula: $Cu_{12}As_4S_{13}$) by the reaction with aqueous $Ca(OH)_2$ is described; in particular a phenomenon whereby high relative concentrations of Ag are formed at the surface following such treatment.

Tetrahedrite-tennantite minerals

Chemistry of the tetrahedrite group

The tetrahedrite group ranges in composition between the end-members tetrahedrite $Cu_{12}Sb_4S_{13}$ and tennantite $Cu_{12}As_4S_{13}$. A variety of substitutions for Cu can occur in the

* E-mail: emhobson@hotmail.com
DOI: 10.1180/0026461067040345

tetrahedrite structure: these include Ag, Fe, Zn, Cd and Hg (Charlat and Levy, 1974; Pattrick and Hall, 1983; Johnson *et al*., 1988; Charnock *et* al., 1989; Ixer and Pattrick, 2003). The cubic structure of these minerals (Fig. 1) is based on the zincblende arrangement (Pauling and Neuman, 1934; Wuensch, 1964) and crystals occur as distinctive tetrahedra. The tetrahedrite group of minerals are an important source of Cu and regularly contain significant Ag concentrations, often several weight percent; consequently, they are also the world's most important primary source of Ag (Ixer and Pattrick, 2003).

The substitutions in the tetrahedrite minerals mean they have amongst the most varied chemistries of all the sulphides. The structure of this group of minerals is such that sites are available for uni-, di- and tri-valent cations, resulting in a general formula in natural tetrahedrite-tennantite species of $M^{+}_{10}M^{2+}_{2}M^{3+}_{4}S^{2-}_{13}$ (see Ixer and Pattrick, 2003). A wide range of intermediate compositions can occur between the tetrahedrite and tennantite end-members, forming a number of solid-solutions. If all the elements found in the tetrahedrite-group minerals are taken into account, the general formula becomes $(Cu,Ag)_{10}(Zn,Mn,Fe,Cd,Cu,Hg)_2(As,Sb,Bi)_4(S,Se)_{13}$ (Ixer and Pattrick, 2003). In tennantites, Ag is almost always only a minor component, or absent due to the incompatibility of large Ag cations in the relatively 'small' tennantite lattice (Charlat and Levy, 1974; Peters, 1977; Pattrick and Hall, 1983; Johnson and Burnham, 1985).

Surface chemistry of the tetrahedrite-group minerals

Currently, information concerning the surface composition and structure of the tetrahedrite group minerals is relatively limited, although data for related phases such as enargite have been presented in recent literature (Pauporte *et al*., 1996; Cordova *et al*., 1997; Velasquez *et al*., 2000*a*,*b*; Ásbjörnsson *et al*., 2004). Analytical work using XPS to determine the surface species of tetrahedrite-tennantite phases has been undertaken by Mielczarski *et al*. (1996*a*,*b*) following conditioning in water, or in an amyl xanthate solution (both kept at pH 10, adjusted by addition of KOH), and tennantite oxidation studies by Fullston *et al*. (1999*a*,*b*) using a KNO_3 solution (pH 11) purged with nitrogen or oxygen gas at 21ºC.

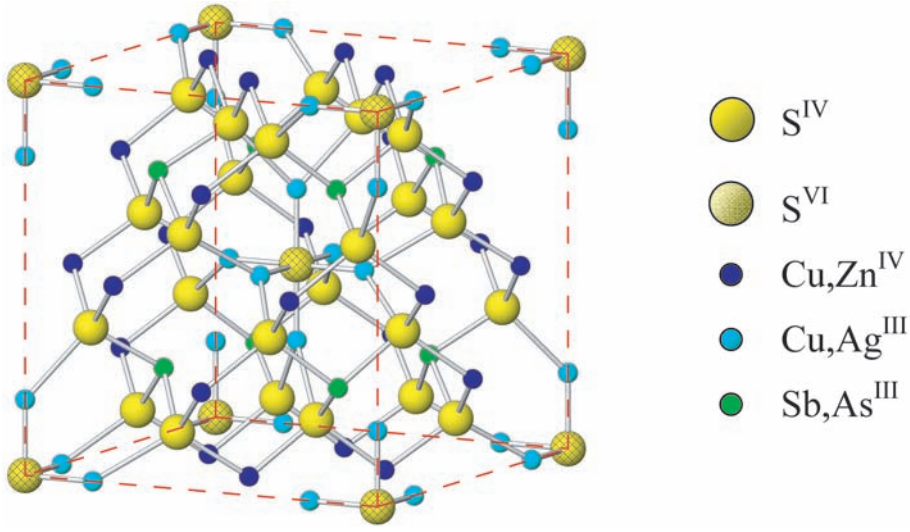

FIG. 1. The half unit-cell structure of the tetrahedrite-group minerals. The tetrahedrite shown in this example has a chemical formula of $Cu_{10}Zn_2Sb_4S_{13}$. The S atoms occupy two sites; the first (S^{IV} site) has four-fold S atoms bonded to the Cu or Zn^{IV} atoms, the second has six-fold S atoms (S^{VI} site) bonded to the Cu or Ag^{III} atoms. Copper also occurs in two sites, a four-fold (Cu^{IV}) site and a three-fold (Cu^{III}) coordinated site. In the case of tennantite from Casapalca, Peru, the Zn^{IV} replaces the Cu^{IV} atoms, and the Ag preferentially replaces the Cu^{III} atoms. Sb or As occur in three-fold coordination adjacent to the vacant site in the structure (from Pattrick and Hall, 1983; after Pauling and Neuman, 1934).

Following treatment in aqueous solution, Mielczarski *et al*. (1996*a*,*b*) observed that the outermost layer of both tetrahedrite and tennantite is oxidized, but the amounts of oxidation products formed at the surface of tennantite were much lower than observed on a tetrahedrite sample. The major surface products formed on tennantite were adsorbed water and metal hydroxides. The XPS data showed there were no Cu2p satellites that would indicate the presence of cupric hydroxide, suggesting only cuprous species were present. Mielczarski *et al*. (1996*a*,*b*) suggested that the products formed at the surface of tennantite subsequent to treatment in an aqueous solution are: (1) a thin outermost layer consisting mostly of cuprous hydroxides, adsorbed water and As hydroxides; (2) an intermediate layer slightly enriched with S; and (3) an inner layer with the composition of the bulk. Fullston *et al*. (1999*a*,*b*) observed similar species at the tennantite surface following treatment in an aqueous solution. Just as in the Mielczarski *et al*. (1996*a*,*b*) studies, Fullston *et al*. (1999*a*,*b*) observed that the surface of tennantite was not heavily oxidized, and was composed of a thin layer of adsorbed water, cuprous and As hydroxides, overlying a S-rich mineral surface.

Surface enrichment of Ag and other trace elements in sulphides has been reported previously in studies of surface oxidation. X-ray photoelectron spectroscopy investigations of bornite (Cu_5FeS_4) were conducted by Buckley and co-authors (1983, 1984, 1985). These studies have shown that exposing bornite to an alkaline solution results in surface species which comprise an Fe oxide/hydroxide, a cupric hydroxide and a Cu sulphide (Buckley and Woods, 1983, 1984; Buckley *et al*., 1984, 1985; Tarasevich *et al*., 2000). Ag is present as a minor element in bornite and Buckley's studies have shown that the concentration of the Ag at the surface relative to the bulk increases dramatically during oxidation, with the Ag segregating into the Cu sulphide layers (Peters, 1977; Buckley and Woods, 1983, 1984; Buckley *et al*., 1984, 1985).

Similar enrichment behaviour to that observed in tetrahedrite, tennantite and bornite has been observed in other sulphides (Buckley and Woods, 1984; Tarasevich *et al*., 2000; Pratesi and Cipriani, 2000). The enrichment of Pb on the surface of galena during exposure to the atmosphere has been reported by Buckley and Woods (1984) and by Buckley *et al*. (1985). The surface species formed during oxidation are Pb hydroxide/oxide and carbonate. Antimony, Cu, Ag and bismuth were present as minor elements in the galena studied, and of these elements, Sb was found to accumulate at the surface achieving a concentration 17 times that of the bulk. Buckley and Woods (1984) suggested that minor elements such as Sb migrate to the oxidized surface in galena, filling Pb vacancies that have been formed through the development of Pb-O species at the air/solid interface (Buckley and Woods, 1984; Buckley *et al*., 1985).

Experimental methods

Samples

A natural end-member tennantite sample from Casapalca, Peru (Table 1) was selected for study and analysed using a CAMECA SX100 Electron Probe Microanalysis (EMPA) instrument, operating at 20 kV accelerated electron potential and 20 nA beam current. The standards used in the analysis were pure Cu, As and Fe metals, synthetic stoichiometric $AgSbS_2$ and ZnS. The identity and purity of the tennantite sample, along with compounds used as standards, were also confirmed by powder X-ray diffractometry (XRD) using a Bruker DA instrument.

Both natural and synthetic Ag samples were used as reference compounds for XPS analysis. The metallic Ag sample was provided by Daresbury Laboratory, and the natural Ag_2S was from the Vtoroy Sovetskiy mine in Russia. Synthetic Ag_2S was produced by reaction between pure (99.999%) Ag and S powders sealed in an evacuated quartz tube and heated in a furnace at 400ºC for 48 h. The resulting crystalline Ag_2S (purity confirmed by XRD) was removed from the quartz tube and crushed to a powder just prior to XPS analysis.

Solution experiments

In order to quantify element leaching from the tennantite caused by the action of a Ca hydroxide ($Ca(OH)_2$) solution, a sample was crushed using an

TABLE 1. Average composition of the studied tennantite from EMPA data (at.% concentrations).

Sample	Cu	Ag	Zn	Sb	As	S	Total
Tennantite	34.1	0.35	5.85	1.2	13.5	44.3	99.2

agate pestle and mortar down to a fine powder. The crushed powder was then placed in a saturated solution of $Ca(OH)_2$ with a pH = 12.4, and agitated. 10 ml aliquots of the solution were removed after 10 min, 30 min, 1 h, 4 h and 8 h and analysed using a Horizon Sequential Inductively Coupled Plasma-Atomic Emission Spectrometry (ICP-AES) instrument which was calibrated using multi-element standards. The aliquots of $Ca(OH)_2$ were analysed for Cu, Ag, As, Sb, Zn and S. The surface area of this powder sample was quantified using the Brunner-Emmet Teller method (BET) which indicated a total area of 0.05 m^2/g.

Surface analysis

Surface analysis by XPS was carried out at the RUSTI Facility, Daresbury Laboratories, Cheshire, UK. The samples for XPS analysis were cleaved in air to produce a face that was representative of the sample, mounted on a sample stub and placed in the XPS loading chamber. This process was carried out in <5 min so as to minimize any oxidation of the freshly cleaved surface. The XPS analysis of untreated samples revealed that the surface of tennantite was particularly resistant to oxidation, with minimal O present (6.3 at.%) on the surface even after 30 min in air. Samples were also analysed in powder form, the powder being placed onto a sample stub and loaded directly into the XPS instrument.

Spectra were recorded using a Scientia ES300 spectrometer with a base pressure of 2.3×10^{-9} mbar, and monochromated Al-$K\alpha$ radiation of 1486.6 eV for excitation of the photoelectrons. The spectrometer employed a hemispherical analyser with constant pass energy of 150 eV. The vacuum pressure inside the chamber was 10^{-8} Pa. The analysis area on the sample surface was ~0.8 mm × 0.2 mm and the take-off angle of the photoelectrons was 90º. The total energy resolution of the machine was less than or equal to 0.33 eV. The analyser was calibrated using elemental references; $Au4f_{7/2}$ (83.7 eV BE), $Ag3d_{5/2}$ (368.3 eV BE), and $Cu2p_{3/2}$ (932.6 eV BE).

Following preliminary XPS analysis, the bulk mineral samples were removed from the instrument, detached from the sample stub, and placed in a saturated solution of $Ca(OH)_2$. The samples were left in $Ca(OH)_2$ solution for between 6 and 12 h, then removed and dried using clean compressed air. The samples were remounted onto the sample blocks and placed back into the XPS instrument for further analysis of the treated cleaved surfaces (no Ca peaks were observed on the treated sample).

The XPS spectra for the depth profiling of the surface of tennantite were recorded at the University of Manchester using a Kratos Axis Ultra spectrometer employing a monochromated Al-$K\alpha$ X-ray source and an analyser pass energy of 80 eV, resulting in a total energy resolution of ~0.55 eV. Uniform charge neutralization of the photo-emitting surface was achieved by exposing the surface to low-energy electrons in a magnetic immersion lens system (Kratos Ltd.). The system base pressure was 5×10^{-10} mbar. Depth profiling was carried out using an Ar^+ ion beam at 5 keV with a target current of 3−5 μA. The analyser was calibrated using elemental references; Au $4f_{7/2}$ (83.98 eV BE), $Ag3d_{5/2}$ 368.26 eV BE) and $Cu2p_{3/2}$ (932.67 eV BE).

The spectral intensities recorded by both the Scientia ES300 spectrometer and the Kratos Axis Ultra spectrometer were converted to surface elemental concentrations by first subtracting a Shirley background (Shirley, 1972) and then obtaining accurate peak positions by fitting peaks using a mixed Gaussian/Lorenzian line shape. The spin orbit components were constrained to have identical elemental spin orbit energy separation, line widths and suitable spin orbital area ratios. All photoelectron binding energies (BE) are referenced to C1s adventitious contamination peaks set at 285 eV BE. Sensitivity factors for the Scientia ES300 spectrometer were taken from the Daresbury Laboratory Scientia Library and for the Kratos Axis Ultra Spectrometer the sensitivity factors were taken from the Scofield Library and a calibrated transmission function.

X-ray absorption spectroscopy (XAS)

To provide complementary data to that yielded by XPS on the structural environment of Ag both in the surface region and in the bulk tennantite, the Ag *L*-edge spectrum of the sample was studied using both Extended X-ray Absorption Fine Structure (EXAFS) spectroscopy of the powdered mineral and reflection EXAFS (REFLEXAFS) analysis of a polished slab. The analyses were carried out on Station 9.3 of the Synchrotron Radiation Source (SRS) at CLRC Daresbury Laboratories. Full details of the procedures involved are given in Pattrick *et al*. (1999). The

TABLE 2. Analysis of the surface of tennantite before and after treatment in a $Ca(OH)_2$ solution for 8 h, as determined by XPS (at.% concentrations).

Sample	Cu	Ag	Zn	Sb	As	S	C	O	Total
Fresh tennantite	18.6	0.3	4.9	0.5	9.9	23.3	37.5	6.3	101.3
Tennantite treated in $Ca(OH)_2$	6.9	10.9	1.1	0.4	5.2	16.6	38.5	20.3	99.9

REFLEXAFS study provides data from the top 50 Å of the sample surface, whereas the EXAFS provides information on the coordination environment of Ag in the whole sample, including the surface.

Results

The EMPA, XRD and XPS data all confirmed the identity of the tennantite (see Tables 1 and 2). The bulk composition obtained by EMPA was very similar to the unreacted surface composition (after the removal of the surface contaminants) obtained by XPS. Optical examination, EMPA and XPS also showed the sample to be chemically homogeneous, with no evidence of other phases being present (although conventional bulk XAS suggested the presence of sub-microscopic Ag sulphide clusters/inclusions; see below).

The XPS analysis of the freshly cleaved surface of the tennantite showed Cu, Ag, Zn, As, Sb and S all to be present (Table 2, Fig. 2). S2p, $Ag3d_{5/2}$, $Sb3d_{5/2}$, $Cu2p_{3/2}$, and $Zn2p_{3/2}$ peak positions are all consistent with metallic sulphides. Cu satellites were not observed in the XPS data suggesting Cu to be present only in the Cu^+ charge state. Arsenic 3d peaks corresponded mainly to sulphide species; however, a small shoulder on the As peak at higher binding energy could represent a minor oxide species.

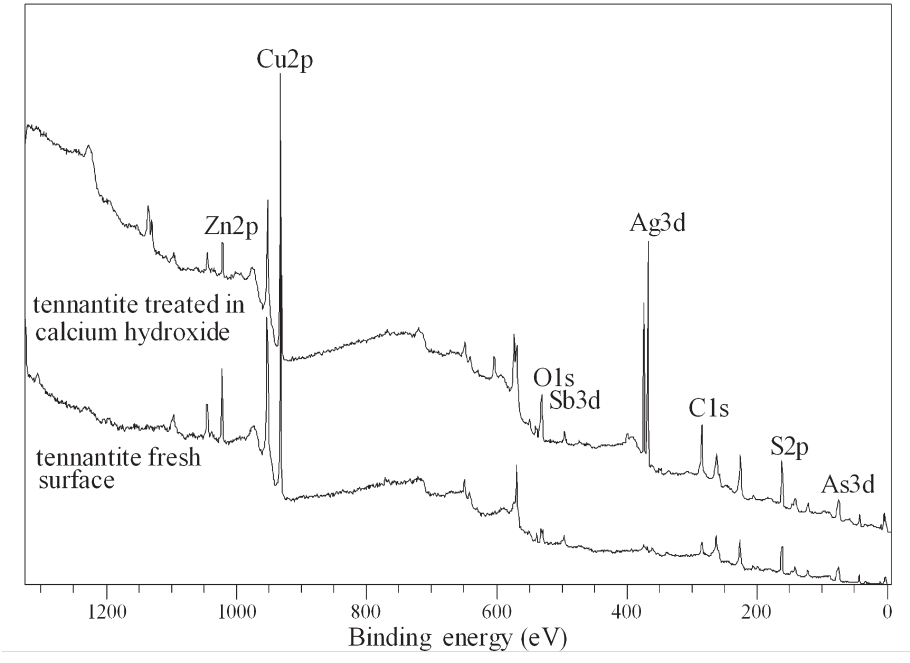

FIG. 2. XPS wide-scan spectra of a freshly cleaved surface of tennantite, and after treatment in $Ca(OH)_2$ solution. The most notable change is the dramatic increase in Ag at the surface following treatment.

TABLE 3. Elemental concentrations as determined by XPS (at.% concentrations) for the surface of treated tennantite before and after depth profiling, showing sputtering times.

Time (min)	Cu	Ag	Zn	Sb	As	S	C	O	Total
0	9.6	20.1	1.3	0.5	4.7	23.5	28.6	11.7	100.0
1	15.9	13.4	5.0	0.6	7.0	33.6	17.9	6.6	100.0
10	19.9	11.8	7.5	0.8	6.6	35.7	11.2	6.5	100.0
30	22.1	10.8	7.9	0.6	6.1	39.5	8.4	4.6	100.0
60	22.5	9.5	8.3	0.6	5.4	39.0	10.0	4.7	100.0
90	23.2	10.2	9.7	0.7	5.3	37.0	9.6	4.3	100.0
120	23.2	9.2	9.9	0.6	5.6	38.6	7.6	5.2	99.9

Oxygen and carbon were also present at the surface (Table 2). These would have arisen through contamination during loading of the sample into the XPS machine and are unavoidable. The C peak, although arising from contamination, is essential for an internal energy calibration reference. One notable feature, however, was the relatively small amount of O found at the surface (6.3%), confirming that tennantite is resistant to oxidation in air compared with many other sulphide minerals (see also Mielczarski *et al*., 1996*a*,*b*; Fullston *et al*., 1999*a*). It should be noted that not all of the O concentrations at the surface maybe associated with oxide/hydroxide species, some are likely to be associated with C species.

As seen from the data presented in Tables 1 and 2, on the untreated surface of tennantite the concentrations of Ag are <0.35 at.%; Cu dominates the M^{+} elements and the M^{2+} element present was Zn, while the M^{3+} elements were dominated by As with a very small amount of Sb. Following treatment in a saturated $Ca(OH)_2$ solution, the surface composition of tennantite changed dramatically (see Fig. 2). The most notable change was that Ag was greatly enhanced in percentage concentration at the treated surface, by up to a factor of 36 times.

The concentrations of both Cu and S at the surface of the tennantite decreased significantly following treatment in $Ca(OH)_2$. There was also a notable change in As and Zn concentrations, As

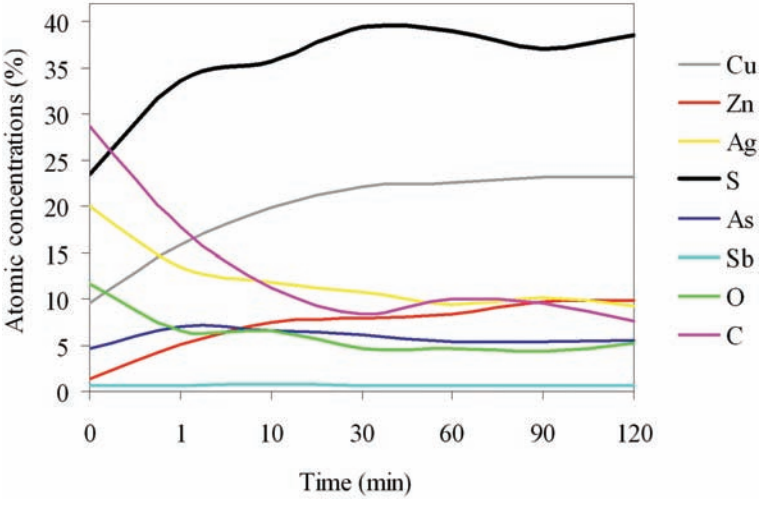

FIG. 3. XPS-determined elemental concentrations for treated tennantite with depth profiling sputtering times (at.% concentrations normalized to 100). The most significant change with depth is the increase in S, Cu and Zn and the decrease in Ag. It must be noted that each point on the horizontal axis denotes a change in concentration with sputtering time on a non-linear scale

decreasing by up to 47% and Zn decreasing by over 78% compared with the fresh surface. The amounts of C and O increased following treatment: this was to be expected during exposure to $Ca(OH)_2$ solution.

Argon ion sputtering to produce an XPS depth profile on a $Ca(OH)_2$ treated sample of tennantite, at 3–5 μA and Ar^+ 5 keV energy, did not completely remove additional Ag from the surface region, even after 2 h. The sample still exhibited higher Ag concentrations than the initial values for the untreated surface (Table 3, Fig. 3). Pratesi and Cipriani (2000) also recorded similar findings, whereby ion sputtering of a tarnished bornite sample did not reach a surface that was representative of the bulk composition. It is not clear whether the Ag concentrations observed here are genuine, or a result from non-uniform sputtering via ion shadowing caused by the rough surface of the tennantite. Variations in Ag, Cu and S intensities between different treated surfaces (Tables 2 and 3) are likely to be a result of the formation of a surface overlayer that is non-uniform in thickness. Depth profiling of the treated sample suggests that the concentrations of Cu, Zn, As and S increase significantly with sputtering, i.e. the concentrations increase with depth. Carbon and O concentrations were reduced significantly with sputtering within the first 1860 s, after which they remained constant.

The XPS peak positions for Ag, Zn, Sb and S do not change following treatment with $Ca(OH)_2$, suggesting that the chemical species remain the same (Buckley *et al.*, 1984). The formation of an O peak at a higher binding energy (532.1 eV) than the expected O1s positions for metal oxides (Moulder *et al*., 1992) could indicate the development of a hydroxide species on the surface of tennantite. The low-intensity As3d peak at 44.2 eV indicates the formation of As oxides (Moulder *et al*., 1992).

It is difficult to index the chemical state of Ag from the $Ag3d_{5/2}$ peak alone because the differences in energy between oxide, sulphide, sulphate and metallic Ag peaks are <0.5 eV (Moulder *et al*., 1992). Therefore, it is necessary to record and compare the positions for both the $Ag3d_{5/2}$ peak and the AgM_5NN Auger parameter. The positions for the $Ag3d_{5/2}$ and AgM_5NN Auger peaks were recorded for the treated surface of tennantite and for Ag metal and Ag sulphide standards (Table 4, Fig. 4*a*,*b*). A comparison was made between the positions recorded for tennantite and those from the Ag standards, and published data on sulphides and oxides (Table 4). The results suggest that the Ag concentrated at the surface of the treated sample is not a metal or an oxide (there is minimal oxidation of the sample); the results are consistent with the surface species being a Ag sulphide. Buckley *et al*., (1984, 1983) concluded from recording the Ag M_4NN and Ag M_5NN Auger parameters for Ag metal, Ag (I) oxide and bornite that the Ag at the surface of bornite is a sulphide species; this is similar to the findings presented here. The XPS depth profiling also reveals that both Cu and As are present at the surface with a Cu + Ag:S ratio of 1:1, similar to that in the fresh tennantite structure. Crucially, however, Zn is no longer present at the surface, distinguishing it chemically from the tennantite. The new species formed at the surface compositionally resembles a cupriferous proustite ($(Cu,Ag)_3AsS_3$) (Table 2 and Fig. 2).

The Ag *L*-edge REFLEXAFS spectra of the polished slabs of untreated tennantite showed just one shell of scatterers around the Ag atom, best fitted as 3S atoms at ~2.50 Å. (Table 5, Fig. 5). After 12 h of treatment with $Ca(OH)_2$, the Ag signal from the tennantite increased significantly in intensity, reflecting an increase in Ag within a layer at the surface of 5 nm, but it was still only possible to resolve one shell of atoms. In contrast, for the bulk EXAFS of the untreated powdered samples (Table 5), a second shell of Ag atoms was discernable at ~2.80 Å, indicating that a proportion of the Ag is present in sub-microscopic Ag-S clusters or inclusions of Ag species. Treatment of the tennantite with $Ca(OH)_2$ for 12 h results in a strong second Ag peak, indicating the development of new Ag species. The X-ray absorption near edge structure (XANES) profiles of all of the samples are very similar, confirming that the bulk of the Ag is in a sulphide phase in all cases. Importantly for this study, it is clear that the Ag is in the form of an Ag sulphide, with a typical Ag–S distance of 2.50 Å; there is no evidence of the presence of significant Ag-O species in any of the treated samples.

ICP-AES data obtained from analysis of the $Ca(OH)_2$ solutions sampled both during and after reaction with tennantite are shown in Fig. 6. The concentrations of both Cu and S in solution are relatively high, 0.6 ppm and 0.9 ppm respectively; small concentrations of Zn were observed in solution (0.1 ppm). However, it must be noted that the concentrations of Zn are at the limits of detection, while Ag, As and Sb were all below the

TABLE 4. Peak positions of the $Ag3d_{5/2}$ photoelectron (BE) and AgM_5NN Auger electron (KE) peaks for the tennantite, and for the Ag standards

Sample	$Ag3d_{5/2}$ (eV)	AgM_5NN (eV)
Tennantite + $Ca(OH)_2$	368.1	350.7
Metallic Ag	368.3	351.8
Ag_2S	368.6	350.7
Ag_2S (syn)	367.8	350.8
AgO	367.4*	356.6*
Ag_2O	367.8*	356.6*

* data published by Gaarenstroom and Winograd (1977)

detection limit. The concentrations of both Cu and S in the alkali solution after 10 min were already high. This was followed by a rapid decrease after the first 30 min and a further gradual decrease between 30 min and 1 h. Concentrations of S increased after the first hour, whereas Cu concentration remained fairly constant. This demonstrates leaching of both Cu and S from the sulphide surface, and some subsequent reprecipitation. Given that Cu solubility is less than that of Zn in hydroxide solutions (data from PHOX; see Polya, 1998) there has probably been selective removal and reprecipitation of Cu at the mineral surface.

The ratio of Cu:Zn:S in solution is consistent with congruent dissolution of the tennantite surface equal to ¼ monolayer of tennantite, but the massive increase in Ag concentration at the surface on tennantite following treatment would require the dissolution of at least 36 monolayers of tennantite. The increased Ag concentration is not consistent with congruent dissolution of the tennantite surface.

Discussion

The enrichment of Ag at the surface of tennantite results in the development of a phase similar to a 'cupriferous proustite' in composition.

To fully understand the nature of the mineral/solution interface it is important to consider the mechanisms of Ag enrichment at the tennantite surface following treatment in an alkaline solution.

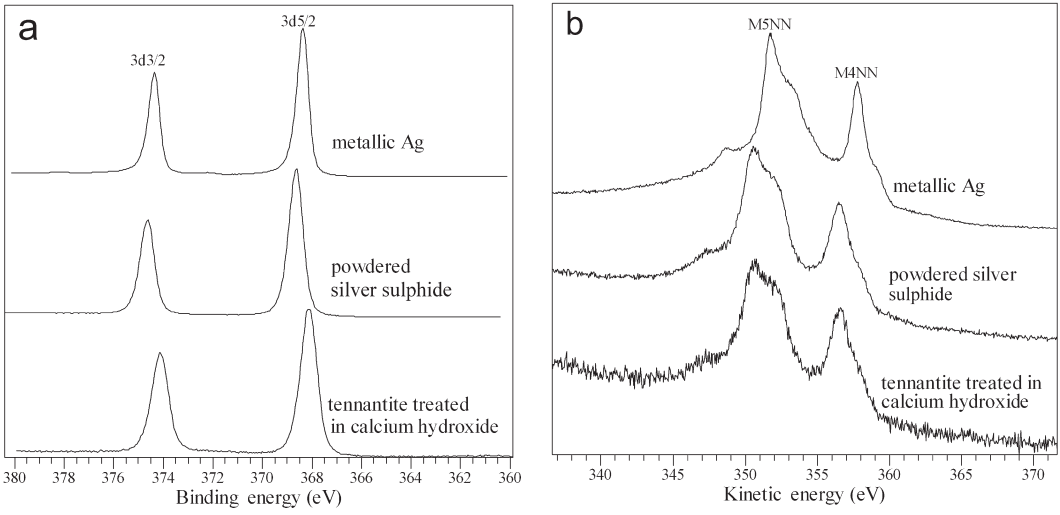

FIG. 4. (*a*) $Ag3d_{3/2}$ and $Ag3d_{5/2}$ XPS peaks for treated tennantite, powdered Ag sulphide and metallic Ag; (*b*) AgM_5NN and AgM_4NN Auger peaks for treated tennantite, powdered Ag sulphide and metallic Ag.

TABLE 5. Summary of the Ag L-edge fluorescence REFLEXAFS data from measurements on a polished sample, and EXAFS data from a ground sample of tennantite before and after treatment in $Ca(OH)_2$ for 12 h.

Sample	Scatterer	N	r (Å)	$2\sigma^2$ (Å^2)	R factor
Tennantite, polished	S	3	2.49	0.026	70.9
Tennantite, polished + $Ca(OH)_2$, 12 h	S	3	2.53	0.029	65.4
Tennantite, ground	S	2	2.51	0.014	56.7
	Ag	2	2.86	0.018	
Tennantite, ground + $Ca(OH)_2$, 12 h	S	2	2.52	0.016	60.0
	Ag	2	2.87	0.023	

N is the number of scatterer atoms at distance r (Å); $2\sigma^2$ is the Debye-Waller factor and R a measure of the goodness of fit.

Previous work on the surface oxidation of tetrahedrite and tennantite by hydroxide solutions suggests that the surface products formed are mainly cuprous and As hydroxides and adsorbed water (Mielczarski *et al*., 1996*a*,*b*; Fullston *et al*., 1999*a*,*b*). The data presented here indicate that the chemical states of surface species are mainly consistent with metal sulphides; however, some hydroxide species are observed at the treated surface.

Mechanisms that could explain the enrichment of Ag at the surface of tennantite include a coupled dissolution/reprecipitation process, or leaching and diffusion. As mentioned above, congruent dissolution alone could not account for the massive Ag enrichment and it would also leave significant Zn either at the surface or in solution, neither of which are observed.

Coupled dissolution/reprecipitation involves dissolving the parent crystal whilst precipitating a new surface species, and also maintaining the parent structure framework. This type of mechanism has been well documented in feldspars (Putnis, 2002; Hellmann *et al*., 2003; Labotka *et al*., 2004). However, to apply this process to tennantite incurs some difficulties. The absence of Zn in the surface layer and in solution would indicate that the mechanism is selective, leaving Zn in the original framework whilst precipitating a new surface species. Though the undissolved component of the tennantite framework might develop into an area rich in ZnS, there is no evidence for such a layer. In any case, once broken down, tennantite is thermodynamically unlikely to recombine as a coherent tennantite lattice (Ebel and Sack, 1994; Ghosal and Sack, 1995; Harlov and Sack, 1995; Sack, 2002, 2005; Wagner *et al*., 2002); it is more likely to reform as secondary binary sulphides.

The solution data show that Cu and S are both leached from the surface of the tennantite. It is well documented that Cu ions are mobile in sulphides (Dutrizac *et al*., 1970; Ugarte and Burkin, 1975; Losch and Monhemius, 1976; Buckley and Woods, 1984; Buckley *et al*., 1984, 1985). A recent computational study by Keith (2002) has shown that within both sphalerite and chalcopyrite lattices, Cu^+ will diffuse more readily than Zn^{2+} or Fe^{3+}. This is because the activation barrier for diffusion of Cu is considerably lower than that of either Zn or Fe. Copper mobility within the tennantite structure is important, as migrating Cu atoms can fill the sites vacated by Ag, stabilizing the bulk (Buckley and Woods, 1984, 1983; Buckley *et al*., 1984, 1985).

The magnitude of the Ag enrichment at the surface of tennantite and the presence of both Cu and S in solution suggest that leaching and a Ag migration mechanism has operated. A driving force for the migration of Ag through the bulk solid to the surface could be the oxidative leaching of Cu, resulting in an unstable metal-depleted surface. This would result in a 'geochemical gradient' that could drive the movement of Ag cations through the bulk to stabilize the surface, similar to the migration mechanisms reported in both bornite and galena (Losch and Monhemius, 1976; Buckley and Woods, 1984; Buckley *et al*., 1984, 1985; Pratesi and Cipriani, 2000).

Leaching of Ag from tetrahedrites with the use of thiourea and thiosulphates has been well documented (Balaz *et al*., 1996, 1998, 2003; Ficeriova *et al*., 2005). Thiourea dramatically dissolves Ag sulphides, resulting in leached Ag being recovered from solution. However, the

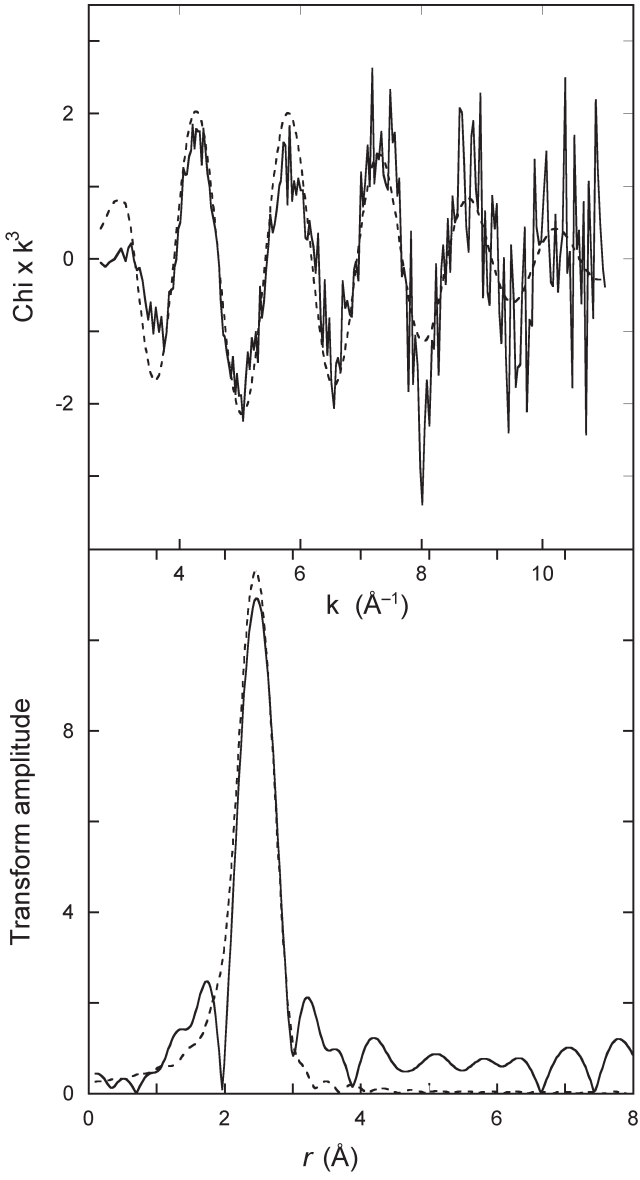

FIG. 5. (*a*) Ag *L*-edge EXAFS spectra (solid line) and theoretical fit (broken line) for tennantite treated in $Ca(OH)_2$ for 12 h; (*b*) Fourier transforms of the Ag *L*-edge EXAFS spectra (solid line) and theoretical fit (broken line) of tennantite treated in $Ca(OH)_2$ for 12 h.

absence of Ag in solution in this study could be explained by the insolubility of Ag in Ca hydroxide solutions.

One possible cause of the selective movement of Ag through the tennantite is the incompatibility of Ag in the tennantite lattice (Charlat and Levy, 1974; Peters, 1977; Pattrick and Hall, 1983; Johnson and Burnham, 1985). The incorporation of the large Ag atoms in tennantite results in lattice strain (Ag has a much larger ionic radius than Cu, the values in four-fold coordination being 1.02 Å and 0.60 Å for Ag^+ and Cu^+, respectively; Shannon and Prewitt, 1970; Shannon, 1976). In addition, Ag substitution

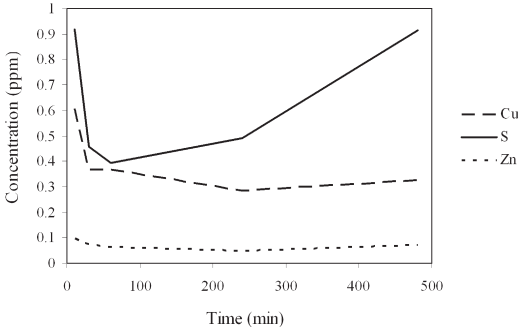

FIG. 6. Concentrations of Cu, S and Zn obtained by ICP-AES for solutions extracted as a function of time during $Ca(OH)_2$ reaction with tennantite. Detection limit for S = 20–50 ppb and for Cu and Zn = 3–5 ppb. Ag, As and Sb were all at or below the detection limit (and hence analysed for but not shown here).

takes place in the trigonal planar site where the metal is bonded to six-fold S in a distorted sphalerite structure. It is not surprising that this site, compared to the more regular tetrahedral sites in the structure, is able both to accommodate and to release relatively large-radius cations.

In sulphides, ion migration is known to occur through a variety of pathways; e.g. via micro-fractures, structural planes and vacancies (Buckley and Woods, 1983, 1984; Buckley *et al*., 1984, 1985, 1989; Lascelles *et al*., 2001; Keith, 2002). All of these mechanisms could contribute to the migration of Cu and Ag from the bulk to the surface of tennantite.

The EXAFS data have provided some evidence of micro Ag-S-Ag cluster rings in the bulk sample although optical and EMPA data indicate homogeneity at least to >1 μm. Either the small amount of Ag present in the tennantite is concentrating in specific trigonal planar sites, or micro Ag-S inclusions are present. The dissolution and diffusion of the latter may have contributed to the surface enrichment.

Following migration, the Ag at the surface could be in one of two forms. Firstly, it could be Ag substituting for Cu in tennantite structural sites at the surface. However, a straight Ag replacement of leached Cu would also leave Zn in the surface layer whereas the surface layer is low in Zn relative to the bulk, and there are only small concentrations of Zn in solution. The depletion of Zn and the limits of Ag substitution (Charlat and Levy, 1974; Peters, 1977; Pattrick and Hall, 1983; Johnson and Burnham, 1985) mean that Ag at the surface is unlikely to be incorporated in a Ag-rich tennantite. Using the data presented here, and previously reported observations (Buckley *et al*., 1984, 1985; Mielczarski *et al*., 1996*a*,*b*; Pratesi and Cipriani, 2000), it appears that a more likely explanation is one where a $(Cu,Ag)_3AsS_3$ phase develops, forming at the oxidized surface, with Ag leached from the tennantite and Ag clusters within the sample.

Ion sputtering of the treated surface of the tennantite resulted in half of the Ag being removed within the first 60 s of bombardment. On the treated surface, the Cu:Ag ratio was initially ~1:2, a substantial enrichment from the untreated surface where the Cu:Ag ratio is 62:1 (Table 2). To accumulate this much Ag from the bulk alone, Ag must have migrated from a depth of at least 9 nm, forming two monolayers of a new phase compositionally equivalent to cupriferous proustite.

Conclusions

This study shows that the treatment of tennantite with a $Ca(OH)_2$ solution dramatically changes the surface chemistry of the mineral, with the development of a phase compositionally similar to cupriferous proustite. The surface properties of tennantite would be modified by the formation of this layer, as would its flotation response. Surface conditioning for the length of time used here would be unlikely in flotation cells, but tennantite with higher concentrations of Ag may behave in this manner, providing another potential complexity to consider in mineral recovery. This enrichment also provides a process for Ag concentration in tennantites that could be exploited in technology.

Acknowledgements

The authors would like to thank Dr J. Charnock (Daresbury), Dr D. Law (RUSTI, Daresbury), Mr D. Plant and Mr P. Lythgoe (Manchester University) for their technical assistance and Prof. A. Putnis for his valuable remarks. This work was funded by an EPSRC scholarship.

References

Ásbjörnsson, J., Kelsall, G.H., Pattrick, R.A.D., Vaughan, D.J., Wincott P.L. and Hope, G.A. (2004) Electrochemical and surface analytical

studies of enargite in acid solution. *Journal of the Electrochemical Society*, **151**, 250–256.

Balaz, P., Ficeriova, J., Sepelak, V. and Kammel, R. (1996) Thiourea leaching of silver from mechanically activated tetrahedrite. *Hydrometallurgy*, **43**, 367–377.

Balaz, P., Achimovcova, M., Ficeriova, J., Kammel, R. and Sepelak, V. (1998) Leaching of antimony and mercury from mechanically activated tetrahedrite $Cu_{12}Sb_4S_{13}$. *Hydrometallurgy*, **47**, 297–307.

Balaz, P., Ficeriova, J. and Villachica, C.L. (2003) Silver leaching from mechanochemically pretreated complex sulfide concentrate. *Hydrometallurgy*, **70**, 113–119.

Buckley, A.N. and Woods, R. (1983) An X-ray photoelectron spectroscopic investigation of the tarnishing of bornite. *Australian Journal of Chemistry*, **36**, 1793–804.

Buckley, A.N. and Woods, R. (1984) An X-ray photoelectron spectroscopic study of the oxidation of galena. *Applications of Surface Science*, **17**, 401–414.

Buckley, A.N., Hamilton, I.C. and Woods, R. (1984) Investigation of the surface oxidation of bornite by linear potential sweep voltammetry and X-ray photoelectron spectroscopy. *Journal of Applied Electrochemistry*„ **14**, 63–74.

Buckley, A.N., Hamilton, I.C. and Woods, R. (1985) Investigation of the surface oxidation of sulfide minerals by linear potential sweep voltammetry and X-ray photoelectron spectroscopy. *Developments in Mineral Processing*, **6**, 41–60.

Buckley, A.N., Woods, R. and Woutherlood, H.J. (1989) An XPS investigation of the surface of natural sphalerites under flotation-related conditions. *International Journal of Mineral Processing*, **26**, 29–49.

Charlat, M. and Levy, C. (1974) Multiple substitutions in the tennantite–tetrahedrite series. *Bulletin de la Societe française de Minéralogie et de Cristallographie*, **97**, 241–250.

Charnock, J.M., Garner, C.D., Pattrick, R.A.D. and Vaughan, D.J. (1989) Coordination sites of metals in tetrahedrite minerals determined by EXAFS. *Journal of Solid State Chemistry*, **82**, 279–289.

Cordova, R., Gomez, H., Real, S.G., Schrebler, R. and Vilche, J.R. (1997) Characterization of natural enargite aqueous solution systems by electrochemical techniques *Journal of the Electrochemical Society*, **144**, 2628–2636.

Dutrizac, J.E., MacDonald, R.J. and Ingraham, T.R. (1970) Kinetics of dissolution of bornite in acidified ferric sulfate solutions. *Metallurgical Transitions*, **1**, 225.

Ebel, D.S. and Sack, R.O. (1994) Experimental determination of the free energy of formation of freibergite fahlore. *Geochimica et Cosmochimica Acta*, **58**, 1237–1242.

Ficeriova, J., Balaz, P. and Boldizarova, E. (2005) Combined mechanochemical and thiosulphate leaching of silver from a complex sulphide concentrate. *International Journal of Mineral Processing*, **76**, 260–265.

Fullston, D., Fornasiero, D. and Ralston, J. (1999*a*) Oxidation of synthetic and natural samples of enargite and tennantite: 1. Dissolution and zeta potential study. *Langmuir*, **15**, 4524–4529.

Fullston, D., Fornasiero, D. and Ralston, J. (1999*b*) Oxidation of synthetic and natural samples of enargite and tennantite: 2. X-ray photoelectron spectroscopic study. *Langmuir*, **15**, 4530–4536.

Gaarenstroom, S.W. and Winograd, N. (1977) Initial and final-state effects in ESCA spectra of cadmium and silver oxides. *Journal of Chemical Physics*, **67**, 3500–3506.

Ghosal, S. and Sack, R.O. (1995) As-Sb energetics in argentian sulfosalts. *Geochimica et Cosmochimica Acta*, **59**, 3573–3579.

Harlov, D.E. and Sack, R.O. (1995) Thermochemistry of Ag_2S-Cu_2S sulfide solutions: Constraints derived from coexisting Sb_2S_3- and As_2S_3- bearing sulfosalts. *Geochimica et Cosmochimica Acta*, **59**, 4351–4365.

Hellmann, R.M., Hervig, R.L., Thomassin, J.H. and Abrioux, M.F. (2003) An EFTEM/HRTEM high-resolution study of the near surface of labradorite feldspar altered at acid pH: evidence for interfacial dissolution-reprecipitation. *Physics and Chemistry of Minerals*, **30**, 192–197.

Ixer, R.A. and Pattrick, R.A.D. (2003) Copper-arsenic ores and Bronze Age mining and metallurgy with special reference to the British Isles. Pp. 9–20 in: *Mining and Metal Production through the Ages* (P. Craddock and J. Lang, editors). British Museum Press, London.

Johnson, M.L. and Burnham, C.W. (1985) Crystal structure refinement of an arsenic-bearing argentian tetrahedrite. *American Mineralogist*, **70**, 165–170.

Johnson, N.E., Craig, J.R. and Rimstidt, J.D. (1988) Crystal chemistry of tetrahedrite. *American Mineralogist*, **73**, 389–397.

Keith, C. (2002) *Computer simulation studies of selected minerals of environmental significance*. PhD Thesis, University of Manchester, UK

Labotka, T.C., Cole, D.R., Fayek, M., Riciputi, L.R. and Stadermann, F.J. (2004) Coupled cation and oxygen-isotope exchange between alkali feldspar and aqueous chloride solution. *American Mineralogist*, **89**, 1822–1825.

Lascelles, D., Sui, C.C., Finch, J.A. and Butler, I.S. (2001) Copper ion mobility in sphalerite activation. *Colloids and Surfaces A – Physicochemical and*

Engineering Aspects, **186**, 163–172.

Losch, W. and Monhemius, A.J. (1976) An AES study of copper-iron sulfide mineral. *Surface Science*, **60**, 196–210.

Mielczarski, J.A., Cases, J.M., Alnot, M. and Ehrhardt, J.J. (1996*a*) XPS characterisation of chalcopyrite, tetrahedrite and tennantite surface products after different conditioning. 1. Aqueous solution at pH10. *Langmuir*, **12**, 2519–2530.

Mielczarski, J.A., Cases, J.M., Alnot, M. and Ehrhardt, J.J. (1996*b*) XPS characterization of chalcopyrite, tetrahedrite, and tennantite surface products after different conditioning. 1. Amyl xanthate solution at pH 10. *Langmuir*, **12**, 2531–2543.

Moulder, J.F., Stickle, W.F., Sobol, P.E. and Bomben, K.D. (1992) *Handbook of X-ray Photoelectron Spectroscopy*. Perkin-Elmer Corporation, USA.

Pattrick, R.A.D. and Hall, A.J. (1983) Silver substitution onto synthetic zinc, cadmium and iron tetrahedrites. *Mineralogical Magazine*, **47**, 441–451.

Pattrick, R.A.D, England, K.E.R., Charnock, J.M. and Mosselmans, J.F.W. (1999) Copper activation of sphalerite and its reaction with xanthate in relation to flotation: an X-ray absorption spectroscopy (reflection extended X-ray absorption fine structure) investigation. *International Journal of Mineral Processing*, **55**, 247–265.

Pauling, L. and Neumann, E.W. (1934) The crystal structure of binnite (Cu, Fe)$_{12}$As$_4$S$_{13}$ and the chemical composition and structure of minerals of the tetrahedrite group. *Zeitschrift für Kristallographie*, **88**, 54–62.

Pauporte, T. and Schuhmann, D. (1996) An electrochemical study of natural enargite under conditions relating to those used in flotation of sulphide minerals. *Colloids Surfaces A – Physicochemical and Engineering Aspects*, **111**, 1–19.

Peters, E. (1977) *Electrochemistry of sulfide minerals*. Pp. 267–290 in: *Trends in Electrochemistry* (J. O'M Bockris, D.A.J. Rand, and B.J. Welch, editors). Plenum Press, New York.

Polya, D.A. (1998) PHOX: Automated calculation of mineral stability and aqueous species predominance fields in Eh (or log ($f_{O(2)}$) or p epsilon)-pH space. *Water-Rock Interaction*, 897–900.

Pratesi, G. and Cipriani, C. (2000) Selective depth analysis of the alteration products of bornite, chalcopyrite and pyrite performed by XPS, AES, RBS. *European Journal of Mineralogy*, **12**, 397–409.

Putnis, A. (2002) Mineral replacement reactions: from macroscopic observations to microscopic mechanisms. *Mineralogical Magazine*, **66**, 689–708.

Sack, R.O. (2000) Internally consistent database for sulfides and sulfosalts in the system Ag_2S-Cu_2S-ZnS-FeS-Sb_2S_3-As_2S_3. *Geochimica et Cosmochimica Acta*, **64**, 3803–3812.

Sack, R.O. (2005) Internally consistent database for sulfides and sulfosalts in the system Ag_2S-Cu_2S-ZnS-FeS-Sb_2S_3-As_2S_3: Update. *Geochimica et Cosmochimica Acta*, **69**, 1157–1164.

Shannon, R.D. (1976) Revised effective ionic radii and systematic studies of interatomic distances in halides and chalcogenides. *Acta Crystallographica*, **A32**, 751–767.

Shannon, R.D. and Prewitt, C.T. (1970) Revised values of effective ionic radii. *Acta Crystallographica*, **B26**, 1046–1048.

Shirley, D.A. (1972) High-resolution X-ray photoemission spectrum of the valence bands of gold. *Physics Review B*, **5**, 4709–4714.

Tarasevich, M.R., Kudaikulova, G.A. and Radyushkina, K.A. (2000) Electroreduction of oxygen on copper-containing sulfide minerals. *Russian Journal of Electrochemistry*, **36**, 49–53.

Ugarte, F.J. and Burkin, A.R. (1975) Mechanism of the formation of idaite from bornite by leaching with ferric sulfate solution. Pp. 46–53 in: *Leaching and Reduction in Hydrometallurgy* (A.R. Burkin, editor). Institution of Mining and Metallurgy, London.

Velasquez, P., Ramos-Barrado, J.R., Cordova, R. and Leinen, D. (2000a) XPS analysis of an electrochemically modified electrode surface of natural enargite. *Surface Interface Analysis*, **30**, 149–153.

Velasquez, P., Leinen, D., Pascual, P., Ramos-Barrado, J.R., Cordova, R., Gomez, H. and Schrebler, R. (2000*b*) SEM, EDX and EIS study of an electrochemically modified electrode surface of natural enargite (Cu_3AsS_4). *Journal of Electroanalytical Chemistry*, **494**, 87–95.

Wagner, T., Boyce, A. and Fallick, A. (2002) Laser combustion analysis of δ^{34}S of sulfosalt minerals: Determining the fractionation systematics and some crystal-chemical considerations. *Geochimica et Cosmochimica Acta*, **66**, 2855–2863.

Wills, B.A. (1997) *Mineral Processing Technology*, 6th edition. Butterworth-Heinemann, Oxford, UK.

Wuensch, B.J. (1964) The crystal structure of tetrahedrite, $Cu_{12}Sb_4S_{13}$. *Zeitschrift für Kristallographie*, **119**, 437–453.

[*Manuscript received 23 May 2005: revised 26 September 2006*]